Int. J. Electrochem. Sci., 7 **(2012)** 8813 - 8831

International Journal of
ELECTROCHEMICAL
SCIENCE
www.electrochemsci.org

Electrochemical and Quantum Chemical Studies on Calmagite and Fast Sulphone Black F dyes as Corrosion Inhibitors for Mild Steel in Hydrochloric Medium

Mwadham M. Kabanda, Sudhish K. Shukla, Ashish K. Singh, Lutendo C. Murulana, Eno E. Ebenso[*]

Department of Chemistry; School of Mathematical and Physical Sciences, North West University (Mafikeng Campus), Private Bag X2046, Mmabatho 2735, South Africa.
[*]E-mail: Eno.Ebenso@nwu.ac.za;

Received: 29 July 2012 / *Accepted:* 24 August 2012 / *Published:* 1 September 2012

The corrosion inhibitive effects of two naphthylazo anionic dyes namely Calmagite (CG) and Fast sulphone black F (FSBF) on mild steel surface in hydrochloric acid solution was studied using electrochemical impedance spectroscopy (EIS),Tafel polarization techniques and quantum chemical calculation methods. Inhibition efficiency increased with increase in concentration of the inhibitors. Trends in the calculated molecular properties (e.g., dipole moment, HOMO and LUMO energies) were compared with trends in the experimentally determined inhibition efficiency. The results show that trends in the quantum chemical descriptors are in agreement with the experimentally determined inhibition efficiencies. The adsorption on the metal surface might be due to both chemisorption and physisorption mechanisms arising from the anionic nature of the molecules in solution (which promote physisorption) and the electron donating effects of the electron rich centres (which promotes chemisorption). The solvent effects have minimal influences on the characteristics of the calculated molecular properties of the dyes.

Keywords: naphthylazo anionic dyes, corrosion inhibitors, chemisorption, physisorption, quantum chemical parameters

1. INTRODUCTION

Metal dissolution impacts negatively on industrial activities because of the damages it causes on the metal-made equipments and the possible contamination of the products by water soluble corrosion by-products. Several approaches have been proposed to minimize or prevent metal dissolution; one of these approaches is the use of substances called corrosion inhibitors [1]. These substances may adsorb physically, chemically or both physically and chemically on the metal surface,

thus blocking and reducing the interaction between the metal surface and the corrosive material [2]. Therefore, an effective corrosion inhibitor should have properties that allow it to physically and chemically adsorb at the metal-solution interface. Such properties are intrinsically contained in the chemical structure of the inhibitor and include properties such as the functional groups present, steric factors, electron density at the adsorption centers and aromaticity or presence of π electrons [3]. Several studies have established that for a series of similar structures, molecules with planar geometry are easily adsorbed on the metal surface than molecular with less planar (more steric) geometry [4]. Studies have also established that molecules with lone pair of electrons, such as heteroatoms, i.e., N, O, S and P and molecules with π electrons prove to have a great tendency to adsorb on the metal surface [5]. This tendency is explained by the fact that systems with high electron density may provide electrons to the partially filled or vacant *d* orbitals of the metal resulting in coordination bonding between the inhibitor and the metal (i.e., resulting in chemical adsorption of the inhibitor on the metal-solution interface).Despite the identification of several classes of compounds as corrosion inhibitors e.g., organic compounds, amino acids, ionic liquids, dyes, etc., the search for effective corrosion inhibitors is an ongoing and an increasing number of classes of compounds are being explored for their corrosion inhibition potentiality in different environments. Although dyes have been extracted from natural sources for centuries, it was not until 1856 that a synthetic dye was produced commercially [6-8]. Different kinds of dyes are known viz. heterocyclic dyes (e.g. safranine T, methylene blue); xanthene dyes (e.g. eosin, thymol blue, phenolphthalein, phenol red) ; anthraquinone dyes (e.g. alixarin red S) and azo dyes (e.g. methyl red, congo red, methyl orange). Of all the dyes, azo dyes are a class of compounds that are strongly coloured. They can be intensely yellow, red, orange, blue or even green, depending on the exact structure of the molecule. Because of their colour, azo compounds are of tremendous importance as dyes. In fact, about half of the dyes in industrial use today are azo dyes, which are mostly prepared from diazonium salts [9]. Structural features in organic compounds that lead to color are >C = C<, -N = O, -N = N-, aromatic rings, >C = O and $–NO_2$. Most importantly, azo (-N = N-) and nitro (-N = O) groups invariably confer colour while the other groups do so under certain circumstances.

Dyes have been used to give multi-colour effects to anodized aluminium [10–15]. Cyanine dyes have been reported as efficient corrosion inhibitors on metal corrodent systems [16]. Green S and erythrosine dyes have been studied as potential inhibitors for mild steel corrosion in HCl [17]. A survey of the literature also reveals that the corrosion on aluminium in amine solutions by some dyes has been reported [18–25]. Preliminary experiments in our laboratories in an earlier study have shown, however, that some azo dyes (metanil yellow, naphthol blue black and solochrome dark blue) actually inhibit the corrosion of mild steel in HCl medium [26]. Some other studies by other research groups and from our laboratories recently reported also show that some organic dyes are quite effective in retarding the corrosion of mild steel and aluminium in acidic or basic environments [27–40]. This study is therefore part of an extensive on-going project in our laboratory to develop new classes of inhibitors from some dyes with good inhibition efficiencies and to further elucidate the mechanism of the inhibition process.

Therefore, in continuation of our interest on the corrosion inhibition characteristics of organic dyes, the present paper reports on the inhibition action of two naphthylazo dyes, namely Calmagite

(CG) and Sulphonate Black F (FSBF) (Fig.1). This is a pair of similar compounds having a naphthylazo moiety and both the sulphonate (SO_3H) and an hydroxyl (-OH) functional groups attached to the naphthylazo moiety. CG has three substituents on the naphthylazo moiety namely a sulphonate group, OH group and an hydroxytoluene group whereas FSBF has three naphthylazo moieties, three sulphonate groups and two hydroxyl groups. The investigations were done by using the electrochemical impedance spectroscopic (EIS), the Tafel polarization and Density functional theory (DFT) method.

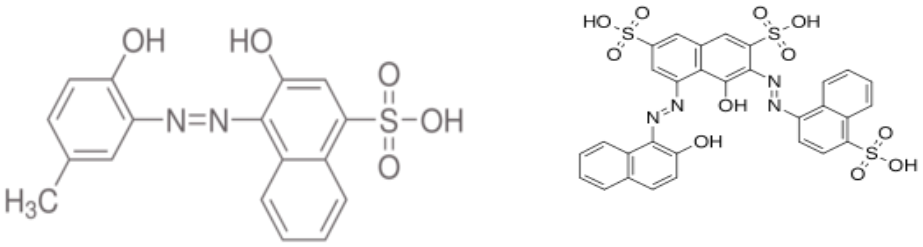

Calmagite (CG) **Fast Sulphone Black F (FSBF)**

Figure 1. Structures of the investigated naphthylazo dyes.

2. EXPERIMENTAL METHODS

Prior to all measurements, the mild steel specimens were abraded successively with emery papers from 600 to 1200 mesh in^{-1}grade. The specimen were washed with double distilled water, degreased with acetone and dried in hot air blower. After drying, the specimen were placed in desiccators and then used for the various experiments. The aggressive solution of 1M HCl was prepared by the dilution of analytical grade hydrochloric acid (37%) with double distilled water and all the experiments were carried out in the unstirred solutions.

The electrochemical measurements were carried out on mild steel strips with the dimension 1.0cm x 1.0cm exposed with a 7.5 cm long stem (coated by the commercially available lacquer).

2.1. Electrochemical impedance spectroscopy

The EIS tests were performed at 303±1K in a three electrode assembly. A saturated calomel electrode was used as a reference and a 1 cm^2 platinum foil was used as counter electrode. All the potentials were measured versus SCE. The electrochemical impedance spectroscopy measurements were perform using a Gamry instrument potentiostat / galvanostat with a Gamry framework system based on ESA 400 in a frequency range 10^{-2}Hz – 10^5 Hz under potentiodynamic conditions with amplitude of 10 mV peak to peak, using AC signal at E_{corr}. Gamry applications include software DC105 for corrosion and EIS300 for EIS measurements and Echem analyst version 5.50 software packages for data fitting. The experiments were carried out after 30 minutes of immersion in the test solution without deaeration and stirring.

The inhibition efficiency of the inhibitor was calculated from the charge transfer resistance values using following equation:

$$\mu_{R_t} = \frac{(1/R_t^o) - (1/R_t^i)}{(1/R_t^o)} \times 100 \quad (1)$$

where R_t^o and R_t^i are the charge transfer resistances in the absence and in presence of inhibitor respectively.

2.2. Potentiodynamic polarization

The electrochemical behavior of mild steel sample in inhibited and non-inhibited solution was studied by recording anodic and cathodic potentiodynamic polarization curves. Measurements were performed in the 1M HCl solution containing different concentrations of the tested inhibitor by changing the electrode potential automatically from −250 to +250mV versus corrosion potential at a scan rate of $1mVs^{-1}$. The linear Tafel segments of anodic and cathodic curves were extrapolated to corrosion potential to obtain corrosion current densities (I_{corr}).

The inhibition efficiency was evaluated from the measured I_{corr} values using the following relationship:

$$\eta_p = \frac{I_{corr}^o - I_{corr}^i}{I_{corr}^o} \times 100 \quad (2)$$

where I_{corr}^o and I_{corr}^i are the corrosion current densities in the absence and presence of inhibitor, respectively.

2.3. Computational details

All geometry optimizations and quantum chemical calculations were performed using density functional theory (DFT) and utilizing the 6–31G(d,p) and 6–31+G(d,p) basis sets. The addition of diffuse functions is considered important for a good description of systems that can form intramolecular hydrogen bonds [41].

The The Becke's Three Parameter Hybrid Functional using the Lee-Yang-Parr correlation functional theory (B3LYP, [42]) was selected for the calculations. DFT/B3LYP is recommended for the study of chemical reactivity and selectivity in terms of the frontier molecular orbitals [43] and other molecular properties such as the electron affinity (EA) and the ionization potential (IP). These molecular properties are often discussed interms of the Koopman's theorem [44, 45]. Electronegativity is estimated by using the equation:

$$\chi \cong -\tfrac{1}{2}\,(E_{HOMO} + E_{LUMO}) \quad (3)$$

Chemical hardness (η) measures the resistance of an atom to a charge transfer [46], it is estimated by using the equation:

$$\eta \cong -\tfrac{1}{2} (E_{HOMO} - E_{LUMO}) \quad (4)$$

Global electrophilicity index (ω) is estimated by using the electronegativity and chemical hardness parameters through the equation:

$$\omega = \frac{\chi^2}{2\eta} \quad (5)$$

Electron polarizability, also called chemical softness (σ), describes the capacity of an atom or group of atoms to receive electrons [46], it is estimated by using the equation:

$$\sigma = 1/\eta \cong -2/(E_{HOMO} - E_{LUMO}) \quad (6)$$

Electron affinity (EA) related to E_{LUMO} through the equation:

$$EA \cong - E_{LUMO} \quad (7)$$

Ionization potential (IP) is related to the energy of the E_{HOMO} through the equation:

$$IP \cong - E_{HOMO} \quad (8)$$

The maximum number of electrons transferred (ΔN_{max}) in a chemical reaction is given by the equation

$$\Delta N_{max} = \frac{\chi}{2\eta} \quad (9)$$

and on using the IP and EA terms can be written as

$$\Delta N_{max} = \frac{(I + A)}{2(I - A)}$$

All calculations were performed by using the Spartan 10 V1.01 program [47]. Schematic structures were drawn using the ChemOffice package in the UltraChem 2010 version while optimized structures were obtained using the Spartan 10 V1.01 program.

3. RESULTS AND DISCUSSIONS

3.1. Potentiodynamic polarization measurements

The potentiodynamic polarization measurements were carried out to study the kinetics of the cathodic and anodic reactions. Figure 2 shows the results of the effect of dyes on the cathodic as well as anodic polarization curves of mild steel in 1M HCl respectively. It is evident from the figure that both reactions were suppressed with the addition of different dyes used in the study. This suggests that all the dyes used in the study reduced the anodic dissolution reactions as well as retarded the hydrogen evolution reactions on the cathodic sites.

Electrochemical corrosion kinetic parameters namely corrosion potential (E_{corr}), corrosion current density (I_{corr}) anodic and cathodic Tafel slopes (b_a and b_c) obtained from the extrapolation of the polarization curves are listed in Table 1.

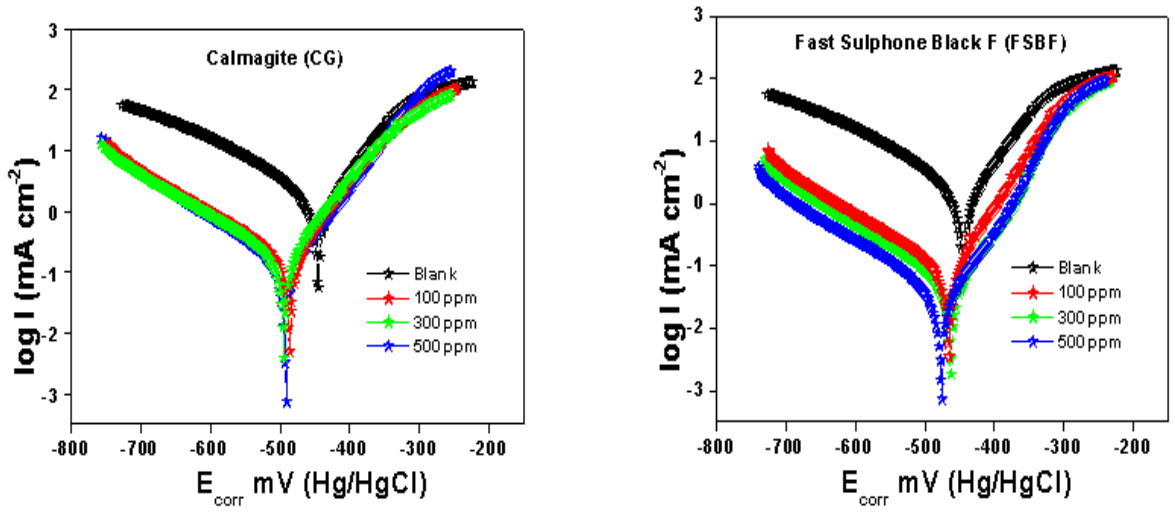

Figure 2. Tafel Polarization Curves for the both dyes with mild steel in 1 M hydrochloric acid solution

Table 1. Tafel polarization data of dyes for mild steel in 1 M HCl solution.

Name of Dye	Conc. of Inhibitor	$-E_{corr}$	I_{corr}	B_a	B_c	IE (%)
–	Blank	448	1400	83	120	-
Calmagite (CG)	100	448	617	72	154	55.9
	300	486	561	76	153	59.9
	500	495	265	69	133	81.1
Fast Sulphone Black F (FSBF)	100	463	534	64	138	61.9
	300	466	351	61	147	74.9
	500	477	199	63	132	85.8

The value of b_c changed with increase in inhibitor concentration and indicates the influence of the inhibitor on the kinetics of the hydrogen evolution. The shift in the anodic Tafel slope, b_a is due to the chloride ion / or inhibitor molecules adsorbed on the metal surface. The corrosion current density (I_{corr}) decreased by the increase in the adsorption of the inhibitor with increasing inhibitor concentration. According to Ferreira *et.al.* [48] and Li *et. al.* [49], if the displacement in corrosion potential is more than 85 mV with respect to the corrosion potential of the blank solution, the inhibitor can be considered as a cathodic or anodic type. In present study, maximum displacement was 40 mV with respect to the corrosion potential of the uninhibited sample which indicates that the studied inhibitor is a mixed type of inhibitor.

3.2. Electrochemical impedance spectroscopy

Electrochemical impedance spectroscopy measurements were carried out in order to study the kinetics of the electrode process and the surface properties of the studied system. This method is widely used to investigate the corrosion inhibition process [50]. Nyquist plots of mild steel in 1M HCl solution in the absence and presence of different concentrations of dyes are shown in Figure 3.

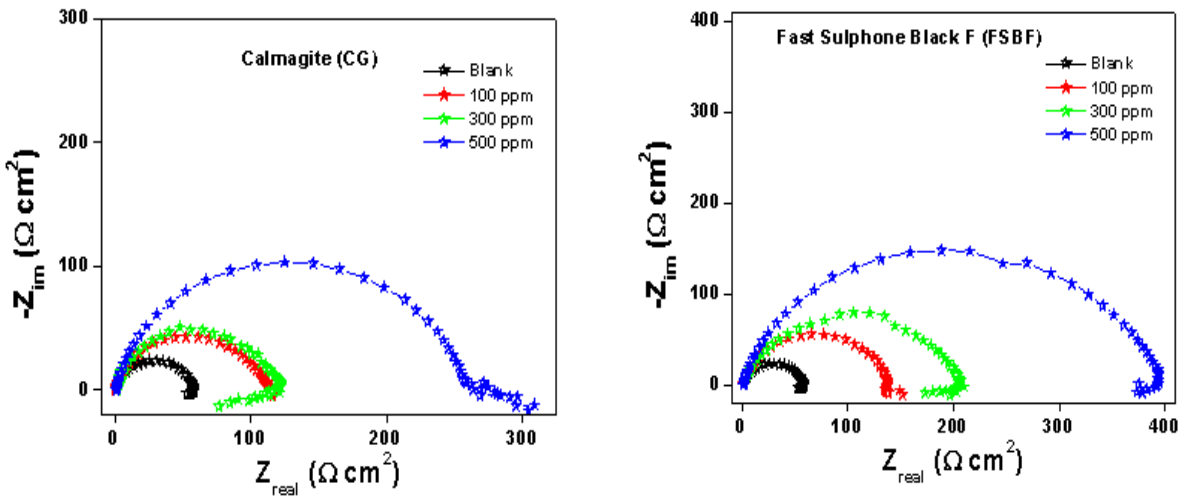

Figure 3. EIS graphs for the dyes with mild steel in 1 M hydrochloric acid solution.

In this plot it is shown that a high frequency depressed charge transfer semicircle is observed. The high frequency semicircle is attributed to the time constant of charge transfer and double layer capacitance [51, 52]. The charge transfer resistance increment raises the tendency of current to pass through the capacitor of the circuit. It is clear from the figure 3 that the impedance spectra is not a perfect semicircle and the depressed capacitive loop corresponds to surface heterogeneity which may be the result of surface roughness, dislocation, distribution of active sites, or adsorption of the different dye molecules[53–55]. The measured data were analyzed using the equivalent circuit shown in figure 4. This circuit is generally used to describe the iron/acid interface model [56]. This circuit gives an

accurate fit to all experimental impedance data for dyes. The equivalent circuit consists of solution resistance (R_s), charge transfer resistance (R_t) and a constant phase angle (CPE).

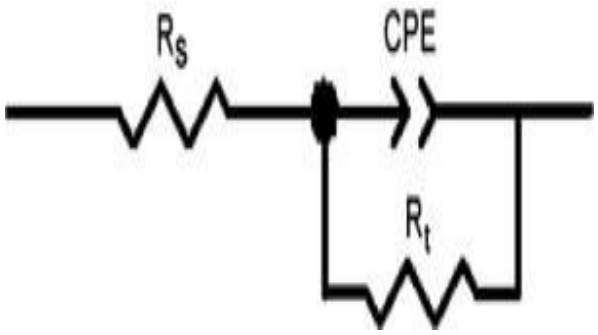

Figure 4. The electrochemical equivalent circuit used to fit the impedance measurements

The impedance function of CPE is as follows:

$$Z_{CPE} = Y^{-1}(j\omega)^{-n} \quad (10)$$

where, *Y* is the magnitude of the CPE, ω is the angular frequency and the deviation parameter *n* is a valuable criterion of the nature of the metal surface and reflects microscopic fluctuations of the surface. For *n*=0, Z_{CPE} represents a resistance with $R=Y^{-1}$; *n*=-1 and inductance with $L=Y^{-1}$ and *n*=1 an ideal capacitor with *C*=*Y* [57]. In iron/steel system ideal capacitor behavior is not observed due to the roughness and /or uneven current distributions on the electrode surface resulting in the frequency depression [58, 59]. The electrochemical parameters R_s, R_t, Y_o and n, for different dyes obtained from the fitting of the recorded data using the equivalent circuit and listed in Table 2. The C_{dl} values listed in Table 2 were derived from the CPE parameters calculated by using the following equation [60].

$$C_{dl} = (Y_o . R_t^{1-n})^{1/n} \quad (11)$$

Table 2. EIS data of the investigated naphthylazo dyes for mild steel in 1 M HCl solution.

Name of Dye	Conc. of Inhibitor	R_s (Ω cm^2)	R_t (Ω cm^2)	Y_0 ($10^{-6}\Omega^{-1}$cm^{-2})	n	C_{dl} (μF cm^{-2})	IE (%)
–	Blank	0.982	50.24	172.0	0.8090	56.02	-
Calmagite (CG)	100	0.874	113.1	145.0	0.7959	50.55	55.6
	300	1.42	121.4	115.4	0.7895	36.99	58.6
	500	1.46	290.5	49.0	0.8018	17.12	82.7
Fast Sulphone Black F (FSBF)	100	1.20	137.8	112.5	0.7990	39.43	63.5
	300	1.26	204.1	95.5	0.7895	33.43	75.4
	500	1.38	394.2	49.1	0.7910	17.32	87.3

It is clear from Table 2 that R_t values increased with increase in the inhibitors concentration. The increase in R_t values is attributed to the formation of the protective film of the inhibitor on metal/solution interface. The values of the double layer capacitance (C_{dl}) decreased with increase in the different dyes. The double layer capacitance (C_{dl}) is related to the thickness of the protective layer (d) by following equation [61].

$$C_{dl} = \frac{\varepsilon \varepsilon_o}{d} \quad (12)$$

where, ε is the dielectric constant of the protective layer and ε_o is the permittivity of the free space. Equation (12) suggests that C_{dl} is inversely proportional to the thickness of the protective layer (d). So the decrease in the double layer capacitance by increasing the inhibitor concentration shows increase in the thickness of protective layer.

It is clear from Table 2 that the dyes inhibited the corrosion of mild steel in 1M HCl solution at every concentration used in the study. The inhibition efficiency (μ_{Rt} %) values listed in Table 2 show that the inhibition efficiency increases with increase in the inhibitor concentration. The results obtained from the EIS studies showed good agreement with the results obtained from the Tafel polarization.

3.3. Results of quantum chemical calculations in vacuo

The schematic representations and the optimized geometries of the two dyes are shown in figure 5.

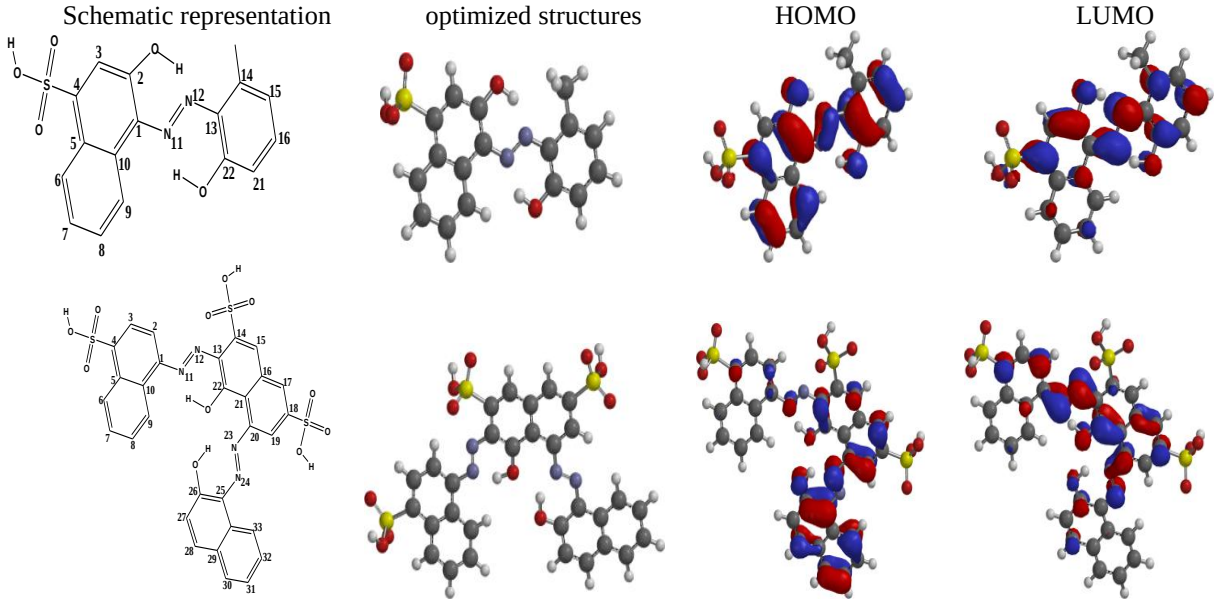

Figure 5. Schematic representation, optimized structures, highest occupied molecular orbital (HOMO) and lowest unoccupied molecular orbital (LUMO) of the studied anionic naphthylazo dyes. DFT/6-31G(d,p) results *in vacuo*. The numbering of the atoms necessary for discussion are shown on the schematic representation.

The numbering of the atoms of interest necessary for discussion is shown on the schematic representation. Only the thermodynamically stable trans state of the azo group was considered for all the structures because this geometry corresponds to planar arrangement of the molecules. All the low-energy conformers of CG and FSBF corresponding to the trans state of the azo group were investigated. These conformers were obtained by optimizing different input geometries prepared through rotation of the C–N, C–C and C–O bonds for each structure. The results show that the low-energy conformers are stabilized by intramolecular hydrogen bond and the conformer with the highest number of intramolecular hydrogen bonds was the most stabilized. A detailed discussion on geometry and total energy of different conformers is beyond the scope of the present work and the discussion throughout this work (on the geometrical parameters, the energies and the quantum chemical parameters) is based solely on the lowest energy conformer of each structure. The bond lengths and bond orders are presented in Table 3 below.

Table 3. Selected bond lengths (Å) and bond order for the studied acidic dyes. B3LYP/6-31G(d,p) results *in vacuo*.

a) Selected bond lengths and bond order in the Calmagite structure

bond	bond length	bond order	bond	bond length	bond order	bond	bond length	bond order
C1-C2	1.409	1.28	C4-C5	1.433	1.17	N12-C13	1.425	1.03
C2-O2	1.335	1.06	C5-C6	1.419	1.31	C13-C14	1.509	1.31
C2-C3	1.416	1.25	C6-C7	1.377	1.52	C14-C15	1.388	1.50
C3-C4	1.371	1.51	C7-C8	1.409	1.33	C15-C16	1.404	1.36
C4-S4	1.799	0.79	C8-C9	1.378	1.51	C16-C21	1.386	1.47
S4-O4′	1.455	1.66	C9-C10	1.417	1.32	C21-C22	1.401	1.37
S4-O4″	1.462	1.69	C1-N11	1.391	1.02	C22-O22	1.340	1.05
S4-O4‴	1.646	0.86	N11-N12	1.288	1.42			

b) Selected bond lengths and bond order in the Fast Sulphonate Black F structure

bond	bond length	bond order	bond	bond length	bond order	bond	bond length	bond order
C1-C2	1.387	1.44	C1-N11	1.408	0.95	S18-O18′	1.462	1.46
C2-C3	1.402	1.31	N11-N12	1.278	1.47	S18-O18″	1.453	1.45
C3-C4	1.381	1.47	N12-C13	1.379	1.08	S18-O18‴	1.645	1.65
C4-S4	1.795	0.80	C13-C14	1.430	1.17	C18-C19	1.395	1.40
S4-O4′	1.462	1.68	C14-S14	1.799	0.78	C19-C20	1.395	1.40
S4-O4″	1.455	1.66	S14-O14′	1.464	1.64	C20-C21	1.441	1.44
S4-O4‴	1.646	0.86	S14-O14″	1.452	1.74	C21-C22	1.441	1.44
C4-C5	1.429	1.21	S14-O14‴	1.645	0.87	C22-O22	1.323	1.32
C5-C6	1.422	1.30	C14-C15	1.361	1.56	C20-N23	1.407	1.41
C6-C7	1.375	1.53	C15-C16	1.429	1.21	N23-N24	1.285	1.29
C7-C8	1.411	1.32	C16-C17	1.410	1.30	N24-C25	1.369	1.37
C8-C9	1.376	1.52	C17-C18	1.380	1.41	C25-C26	1.424	1.42
C9-C10	1.420	1.29	C18-S18	1.793	0.79	C26-O26	1.325	1.33

The C–C bond lengths (Å) of the substituted naphthalene ring are in the range 1.371-1.433 for CG and 1.375–1.429 for FSBF. These ranges are comparable to the range of the calculated and experimental bond lengths in the isolated naphthalene reported in literature [62]. The longest bond lengths correspond to the C-S and S–O(sp^3) bonds. These bonds also correspond to the weakest bonds (lowest values of the bond order) in the studied systems. The S–O(sp^2) are also longer (and therefore weaker) than the C–C bond. The C–N bond lengths are relatively closer to the C–C bond length while the N–N is the shortest. The N–N bond length also has the highest bond order value and therefore it is the strongest. The optimized geometries have a planar arrangement with the exception of the O atoms of the sulphonate group and the methyl H atoms in CG. The intramolecular hydrogen bonds results in the formation of two 6 membered rings in Calmagite; two 6 membered rings and one 10 membered ring in sulphone Black F.

The chemical reactivity of molecules is often discussed in term of quantum chemical parameters such as the Highest occupied molecular orbital (HOMO), the lowest unoccupied molecular orbital (LUMO), the energy of the Highest occupied molecular orbital (E_{HOMO}), the energy of the lowest unoccupied molecular orbitals (E_{LUMO}) and electron density parameters such as the dipole moment (D), partial charges on the atoms, etc. Such quantities, and many others, provide qualitative information on the distribution of charge in the molecule and the electron density from which it is possible to discuss the reactivity and selectivity of molecular systems.

Table 4. Calculated molecular properties for Calmagite (CG) and Fast Sulphone Black F (FSBF).

Quantum chemical properties	B3LYP/6-31G(d,p) results		B3LYP/6-31+G(d,p) results	
	CG	FSBF	CG	FSBF
Energy (au)	–1539.99871	–3396.07023	–1540.04201	–3396.15269
E_{HOMO} (eV)	–5.936	–5.973	–6.283	–6.286
E_{LUMO} (eV)	–3.041	–3.586	–3.384	–3.911
ΔE (eV)	2.895	2.387	2.898	2.375
μ (Debye)	4.90	5.33	5.35	6.52
Molecular area (A^2)	337.40	609.33	337.73	610.90
Molecular volume (A^3)	323.18	590.48	323.51	591.28
Polarizability	66.91	40.81	66.93	40.81
HBD count	2	2	2	2
HBA count	4	6	4	6
Ionization potential, I (eV)	5.936	5.973	6.283	6.286
Electron affinity, A (eV)	3.041	3.586	3.384	3.911
Electronegativity (χ)	4.489	4.779	4.834	5.098
Hardness (η)	1.447	1.193	1.449	1.188
Softness (σ)	0.691	0.838	0.690	0.842
Fraction of electrons transferred (ΔN)	–0.867	–0.930	–0.747	–0.801
Electrophilicity (ω)	6.961	9.571	8.061	10.944

The calculated quantum chemical parameters necessary for discussion on the reactivity of the selected are reported in table 4. The HOMO and the LUMO orbitals of the studied dyes are also shown in figure 5. In CG, the HOMO is delocalized throughout the molecule except on the sulphonate and methyl group while in FSBF, the HOMO is delocalized strongly on the ring attached to N24 with the sulphonate groups being completely excluded. The HOMO in FSBF also excludes the N11-N12 atoms. These results suggest that the sulphonate group has a less tendency to donate electrons. The LUMO is also delocalized in certain regions of the molecules; in structure CG, the LUMO is strongly delocalized in the phenyl hydroxyl group and in the azo group regions; in structure FSBF the LUMO is delocalized on the N11–N12 azo group and on the C22 carbon atom.The energy of the HOMO (E_{HOMO}) represents the ability of the molecule to donate a lone pair of electrons and the higher the E_{HOMO} value, the greater the tendency of the molecule to donate electrons to an electrophilic reagent [62]. The results show that E_{HOMO} follows the order CG > FSBF. E_{LUMO} represent the ability of the molecule to accept electrons from a donor reagent and the lower the E_{LUMO} is, the greater the tendency of the molecule to accept electrons. Results from Table 4 show that E_{LUMO} decreases in the order FSBF < CG.

The energy difference between E_{HOMO} and E_{LUMO} (i.e., ΔE) informs of the reactivity of the given compound; the smaller the ΔE value, the greater the reactivity of the molecule. The results show that FSBF has the smallest ΔE value and is therefore the most reactive molecule. In this way FSBF would readily adsorb on the metal surface resulting in greater inhibition efficiency, what is in agreement with experimentally reported inhibition efficiencies.

The dipole moment gives information on the polarity (the hydrophobicity) of a molecule and therefore the electron distribution in the molecule. The higher the dipole moment is, the higher is the polarity of the molecule. In the study of corrosion inhibition, two different trends are often sighted correlating dipole moment with the IE; inhibition efficiency has been reported to increase with increase in the dipole moment of the inhibitor [2], in other reports, inhibition efficiency has been reported to increase with the decrease in the dipole moment of the inhibitor [63], Yet again there are instances in which the dipole moment of the inhibitor has not shown any correlation to the inhibition efficiency of the inhibitor [3]. In the current work the order of inhibition efficiency is such that FSBF < CG, which implies that inhibition efficiency increases with the decreased in the dipole moment of the molecules.

Like dipole moment, molecular polarizability gives information on the electron distribution and therefore the reactivity of the molecule. Molecules whose electron cloud is easily distorted have a low polarizability value while molecule whose electron cloud is not easily distorted have a very high polarizability value. Molecules with low polarizability values are therefore more reactive than molecule with high polarizability value. In the current study the order of polarizability is such that FSBF < CG, which is in agreement with experimentally reported inhibition efficiency.

Molecular volume is another quantity that has been related to the inhibition efficiency of an inhibitor. Higher molecular volume implies greater contact between the inhibitor and the metal surface. However, it is important that the planarity of the studied inhibitor be taken into consideration when discussing the molecular volume because in cases where the molecule volume is high but the molecule is less planar it may still be observed that the IE is lower. In the current study the molecular volume

has been found to follow the order FSBF > CG, which is also in agreement with experimentally determined inhibition efficiency.

Other quantities that are often sighted in the discussion of the reactivity of molecule include the ionization potential, electronegativity (χ), global hardness (η), global softness (σ), fraction of electrons transferred (ΔN) and electrophilicity (ω). Ionization potential is the amount of energy required to remove an electron from a molecule. The lower the ionization potential the easier it is to remove an electron from a molecule. In the current study, the ionization potential increases in the order CG < FSBF.

Global hardness and softness parameters are related to the description of the hard and soft acid/base through the acid-based theory [64]. A hard molecule has the least tendency to react while a soft molecule has high tendency to react. The order of softness is such that FSBF > CG. This trend is also in agreement with experimentally determined inhibition efficiency.

A comparison of the fraction of electrons transferred show that FSBF has the highest tendency to transfer electrons. This result may explain why FSBF has the highest tendency to reactivity, because the fraction of electrons transferred is an indication of reactivity. It is reasonable to infer that FSBF would have the highest inhibition efficiency which agrees with experimentally observed inhibition efficiency.

Electrophilicity values gives information on the nucleophilic or electrophilic nature of the molecule. A high electrophilic value informs that the molecule has a high tendency to act as an electrophile while a low value of electrophilicity informs that the molecule has a high tendency to act as a nucleophile. The order of the electrophilicity values is such that FSBF > CG. This trend also agrees with experimental results.

The charges on the atoms also gives information on the electron distribution in the molecule and therefore the reactivity of a molecule. It also informs of the selectivity of the molecule i.e., the specific centers on the molecule for which a certain type of reactions is likely to occur. Centers with the highest negative charge in the molecule are often susceptible to an electrophilic attack [65]. Table 5 reports the Mulliken atomic charges for the non-hydrogen atoms of the studied molecules.

Table 5. Mulliken atomic charges (*e*) for the selected atoms of the studied acidic dyes (Results *in vacuo*)

a) Mulliken atomic charges on selected atom of structure CG

B3LYP/6-31G(d,p)						B3LYP/6-31+G(d,p)					
atom	charge	atom	charge	atom	charge	atom	charge	atom	charge	atom	charge
C1	0.230	S4	1.265	N12	–0.413	C1	–0.031	S4	1.604	N12	–0.191
C2	0.354	C5	0.107	C13	–0.230	C2	0.353	C5	0.153	C13	0.209
O2	–0.565	C6	–0.133	C14	0.118	O2	–0.563	C6	–0.190	C14	0.386
C3	–0.130	C7	–0.098	C15	–0.151	C3	–0.247	C7	–0.030	C15	–0.325
C4	–0.254	C8	–0.086	C16	–0.070	C4	–0.622	C8	–0.091	C16	–0.207
O4′	–0.502	C9	–0.112	C21	–0.123	O4′	–0.488	C9	–0.283	C21	–0.257
O4″	–0.520	C10	0.079	C22	0.357	O4″	–0.582	C10	0.166	C22	0.309
O4‴	–0.568	N11	–0.423	O22	–0.573	O4‴	–0.590	N11	–0.141	O22	–0.537

b) Mulliken atomic charges on selected atom of structure FSBF

B3LYP/6-31G(d,p)						B3LYP/6-31+G(d,p)					
atom	charge	atom	charge	atom	charge	atom	charge	atom	charge	atom	charge
C1	0.248	C10	0.094	O18′	–0.485	C1	0.057	C10	0.140	O18′	–0.502
C2	–0.066	N11	–0.448	O18″	–0.524	C2	–0.106	N11	–0.148	O18″	–0.559
C3	–0.122	N12	–0.303	O18‴	–0.549	C3	–0.009	N12	0.072	O18‴	–0.548
C4	–0.248	C13	0.279	S18	1.223	C4	–0.941	C13	0.097	S18	1.697
O4′	–0.520	C14	–0.249	C19	–0.058	O4′	–0.483	C14	–0.643	C19	–0.085
O4″	–0.505	O14′	–0.481	C20	0.265	O4″	–0.577	O14′	–0.500	C20	–0.098
O4‴	–0.568	O14″	–0.529	C21	0.090	O4‴	–0.587	O14″	–0.606	C21	0.070
S4	1.262	O14‴	–0.564	C22	0.336	S4	1.636	O14‴	–0.612	C22	0.150
C5	0.103	S14	1.267	O22	–0.575	C5	0.167	S14	1.734	O22	–0.625
C6	–0.130	C15	–0.141	N23	–0.449	C6	–0.165	C15	–0.303	N23	–0.169
C7	–0.093	C16	0.084	N24	–0.312	C7	–0.117	C16	0.206	N24	–0.029
C8	–0.088	C17	–0.131	C25	0.194	C8	–0.157	C17	–0.096	C25	0.318
C9	–0.111	C18	–0.206	O26	0.566	C9	–0.119	C18	–0.809	O26	–0.550

The results show that O atoms have the highest negative charge, followed by the N atoms (O is more electronegative than N and therefore has the greatest tendency to attract electrons towards itself). These atoms are therefore likely to take part in an electrophilic attack in which case they will readily donate electrons to the electrophilic species. When the electrophilic species is the metal surface, the donated electrons are accepted in the partially filled or vacant *d* orbitals of the metal, which allows the molecules to be adsorbed on the metal surface, in a chemisorption process. These results are in agreement with the electron density potential surface, showing that O atoms and N atoms are susceptible to electrophilic attack. All C atoms directly attached to N and O atoms are electron deficient (i.e., they have positive charge) and therefore could be subject to nucleophilic attack, also all S atoms are strongly electron deficient.

The other quantum chemical parameters that are often utilized in the prediction of the selectivity of molecule is the Fukui condensed functions. The Fukui function, F(r) is defined as the derivative of the electronic density (ρ) with respect to the number of electrons N at a constant external potential (υ)[66], i,e.,

$$f = (\delta\rho(r)/\delta N) \qquad (4)$$

Fukui functions are often used to locate regions in the molecule that are susceptible to electrophilic or nucleophilic attack. When defined in terms of the charges on the atoms the electrophilic attack and the nucleophilic attack terms could be estimated utilizing the finite difference approximation approach as follows [66]:

$$f^{+} = q_{(N+1)} - q_N \qquad \text{for a nucleophilic attack} \qquad (13)$$

$$f^{-} = q_N - q_{(N-1)} \qquad \text{for an electrophilc attack} \qquad (14)$$

where $q_{(N+1)}$, q and $q_{(N-1)}$ are the charges of the atoms on the systems with N+1, N and N–1 electrons respectively. The preferred site for nucleophilic attack is the atom or region in the molecule where the value of f^+ is the highest and the preferred site for an electrophilic attack is the atom/region in the molecule where the value of f^- is the highest. The calculated Fukui condensed functions are reported in Table 6; the highest value of f^+ is on C7 and O22 in CG and O26 in FSBF; the highest values of f^- is on O2 and O22 in CG and C5 and O26 in FSBF.

3.4. Results of the calculations in water solution

Table 6. Calculated condensed Fukui functions the selected atoms of the studied acidic dyes. B3LYP/6-31G(d,p) results *in vacuo*.

Fast Sulphone Black F			Calmagite		
atom	f^-	f^+		f^-	f^+
C1	–0.005	0.003	C1	–0.049	–0.006
C2	–0.020	–0.025	C2	–0.031	–0.035
C3	–0.003	0.000	O2	–0.058	–0.042
C4	–0.023	–0.025	C3	–0.009	–0.016
O4′	–0.030	–0.003	C4	–0.030	–0.040
O4″	–0.002	–0.034	O4′	–0.027	–0.026
O4‴	–0.006	–0.007	O4″	–0.025	–0.027
S4	–0.016	–0.023	O4‴	–0.008	–0.011
C5	0.203	0.001	S4	–0.025	–0.039
C6	–0.013	–0.009	C5	–0.002	0.005
C7	–0.005	–0.005	C6	–0.022	–0.012
C8	–0.010	–0.010	C7	–0.023	–0.158
C9	–0.010	–0.001	C8	–0.011	–0.014
C10	–0.009	–0.014	C9	–0.029	–0.002
N11	–0.014	–0.037	C10	–0.001	–0.020
N12	–0.006	–0.053	N11	–0.002	–0.054
C13	–0.022	0.001	N12	–0.013	–0.065
C14	–0.006	–0.007	C13	–0.035	0.004
O14′	–0.011	–0.009	C14	–0.004	–0.018
O14″	–0.016	–0.019	C15	–0.022	–0.006
O14‴	0.000	0.005	C16	–0.018	–0.025
S14	–0.015	–0.019	C21	–0.014	–0.010
C15	–0.018	–0.012	C22	–0.023	–0.033
C16	0.006	0.000	O22	–0.052	–0.155
C17	–0.026	–0.017			
C18	–0.004	–0.016			
O18′	0.022	–0.057			
O18″	–0.050	0.024			
O18‴	–0.004	–0.006			
S18	–0.015	–0.021			
C19	–0.025	–0.007			
C20	–0.008	–0.028			
C21	–0.008	–0.007			
C22	–0.013	–0.038			
O22	–0.003	–0.021			
N23	–0.018	0.005			
N24	–0.004	–0.033			
C25	–0.195	–0.004			
O26	1.103	–1.145			

The inclusion of solvent effects in the computational study of inhibitor is significant in consideration of the fact that electrochemical reactions take place in solution. In this ways the results in solution is expected to provide more realistic trends to the experimental results. Only single point calculations were performed because of the computational demands of optimizing FSBF in water solution. Single point calculations provide molecular parameters in solution at the same geometry as *in vacuo*.

One of the most important quantities when considering the results in solution is the free energy of solvation (ΔG_{solv}). It gives information on the extent by which the inhibitor is solvated. The large values of ΔG_{solv} suggest that the inhibitor is highly solvated while small values of ΔG_{solv} suggest that the solvent is partially solvated. Molecules that strongly dissolve in water solution are less effective as inhibitors while molecules that have small ΔG_{solv} are highly effective as inhibitors. A comparison of the solvation energy values for the calculated acidic dyes (Table 7) show that the trend is such that CG < FSBF, which suggests that CG would have the least tendency to dissolve in water solution and the highest tendency to adsorb on the metal surface. This trend however does not agree well with experimentally determined inhibition efficiency.

Table 7. The molecular properties for Calmagite (CG) and Fast Sulphone Black F (FSBF) obtained through SM8 single point calculations on the input geometry optimized *in vacuo* (B3LYP/6-31G(d,p) results in water solution).

Structure %IE[b]	Quantum				chemical								properties[a]
	ΔG_{solv}	E_{HOMO}	E_{LUMO}	ΔE	μ	IP	EA	χ	η	σ	ΔN	ω	
CG	–6.51	–5.854	–2.941	2.913	6.31	5.854	2.941	4.397	1.456	0.687	–0.894	6.638	63.3
FSBF	–15.82	–5.779	–3.412	2.367	6.128	5.779	3.412	4.595	1.184	0.845	–1.016	8.921	74.2

[a] solvent effect (ΔG_{solv}) is in kcal/mol; E_{HOMO}, E_{LUMO}, ΔE, ionization potential (IP) and electron affinity (EA) are in eV; diploe moment (μ) is in debye. η is the global hardness, σ is the global softness, ΔN is the total number of electrons transferred and ω is the electrophilicity index.
[b] experimental inhibition efficiencies (%IE) are included for comparison purposes

A comparison of the molecule properties in water solution show interesting patterns: the E_{HOMO} values show that FBSF has the highest tendency donate electrons; the E_{LUMO} values follows the order FSBF > CG; the values of ΔE follow the order FSBF > CG. All these trends suggest that FSBF has the highest tendency to interact with the metal surface (and therefore adsorb onto the metal surface). A comparison of the global softness and the number of electrons transferred (ΔN) also confirms that FSBF is a better corrosion inhibitor than CG. Collectively, all the results agree well with the experimental results. A comparison of the molecular properties across media suggests increased electron donating ability of the inhibitors; the HOMO is higher in water solution, indicating an increased electron donating ability of the inhibitors; the LUMO is increased in water solution indicating the decreased tendency of the inhibitor to act as electron acceptor; ΔN is higher in water solution, indicating the ability of the molecule to transfer electrons is higher in water solution than *in*

vacuo; the electrophilicity index is smaller in water solution than *in vacuo*, indicating that the ability of the molecule to acts as electron donor (nucleophile) is higher in water solution than *in vacuo.* Therefore the solvent effect has a tendency to increase the ability of the anionic dyes to interact with metal surface by donating electrons to the partially filled or vacant *d* orbitals of the metal.

4. CONCLUSIONS

Electrochemical impedance spectroscopic (EIS) , the Tafel polarization and Density functional theory (DFT) methods were employed in the investigation of the inhibitive potentiality of Calmagite and Fast sulphone black F towards the corrosion of mild steel in acidic medium. The main conclusions of the work are as follows:

i. Both dyes are effective corrosion inhibitors; however Fast Sulphone Black F has higher inhibition efficiency than Calmagite.

ii. An increase in the inhibitors concentration causes increased the inhibition efficiency.

iii. The trends in some quantum chemical parameters for the calculation *in vacuo* as well as in water solution show good correlation with the trends in the experimental inhibition efficiencies with FSBF having the highest inhibition efficiency.

iv. Potentiodynamic polarization studies showed that both dyes exhibited mixed-type interaction mechanism (i.e., both chemisorption and physisorption mechanisms of interaction).

v. Physical adsorption may arise from the electrostatic attraction between the negative charge of the inhibitor and the positive charge of the metal; chemical adsorption may arise from possible interactions between the electron donor centers in the inhibitor and the partially filled or vacant *s* or *d* orbitals of the metal.

ACKNOWLEDGEMENTS
M. M. Kabanda, Ashish K. Singh and Sudhish K. Shukla are grateful to the North-West University for granting them Postdoctoral Fellowships.

References

1. P. C. Okafor, E. E. Ebenso, U. J. Ekpe, *Int. J. Electrochem.* Sci. 5 (2010) 978.
2. N. O. Eddy, F. E. Awe, C. E. Gimba, N. O. Ibisi, E. E. Ebenso, *Int. J. Electrochem. Sci*., 6 (2011) 931.
3. N. O. Obi-Egbedi, I. B. Obot, M. I. El-Khaiary, S. A. Umoren, E. E. Ebenso, *Int. J. Electrochem. Sci.*, 6 (2011) 5649.
4. F. Bentiss, M, *J. Mater. Environ. Sci*. 2 (2011) 13.
5. J.G.N. Thomas, in: Proceedings of the fifth European symposium on corrosion inhibitors, Ann. Univ. Ferrara., Italy, 1980–1981, p. 453.
6. I.N. Putilova, V.P. Barranik, S.A. Balezin, in Metallic Corrosion Inhibitors, Bishop, E. (ed). Pergamon Press, Oxford (1960) p31.
7. K. Venkataraman, The Chemistry of Synthetic Dyes, Academic Press, New York (1970) p.31.
8. K. Venkataraman, The Chemistry of Synthetic Dyes, Academic Press, New York (1970) p.311.

9. J.D. Roberts, M.C. Caserio, Basic Principles of Organic Chemistry 2nd ed. W.A. Benjamin Inc., California (1979).
10. J.D. Talati, D.K. Gandhi, *Werkst. Korros*. 33(1982) 195.
11. J.D. Talati, D.K. Gandhi, *Indian J. Technol*. 30 (1982) 312.
12. J.D. Talati, D.K. Gandhi, *Corrosion 4*0 (1984) 88.
13. J.D Talati, J.M. Daraji, *Trans. SAEST*. 21 (1980) 41.
14. J.D Talati, J.M. Daraji, *Electrochem. Soc. India* 35 (1986) 175.
15. J.D Talati, J.M. Daraji, *J. Indian Chem. Soc*. 65 (1988) 94.
16. M.Th. Maklouf, G.K. Gomma, M.H. Wahdan and Z.H. Khalil, *Mater. Chem. Phys.* 40 (1995) 119.
17. B.I. Ita, C.A. Edem, *C.A. Global J. Pure and Appl. Sci*. 6 (2000) 239.
18. A.Bukowiecki, *Werkst. Korros*. 10 (1959) 91.
19. H. Kato, Y. Hayakama, *Denki Kagaku* 38 (1970) 9.
20. H. Kotono, F. Tanimoto, Y. Aizawa, T.Karamoto, Jpn Patent 7367, 142(1974) [*Chem.Abstr*. 80(1974) 18568c].
21. C. Yashimura, M. Iwaseki, *Aruminyunu Kenkyu Kaishi* 22 (1977) 76.
22. H.Yameda, M.Yoshizawa, T. Okamoto, Jpn Patent 7260, 496(1974) [*Chem.Abstr*. 80(1974) 18568c].
23. J.D. Talati, J.G.A. Patel, *Br. Corros. J*. 9 (1974) 181.
24. J.D. Talati, J.M. Pandya, *Anti-Corros. Methods. Mater*. 20 (1974) 7.
25. J.D. Talati, N.H. Joshi, *Werskt. Korros.* 3 (1980) 926.
26. E.E. Ebenso, Niger. *Jour. Chem. Res.* 6 (2001) 8.
27. L. Tang, G. Mu, G. Liu, *Corros. Sci.* 45 (2003) 2251.
28. L.Tang, X. Li, G. Mu, G. Liu, *Appl. Surf. Sci.* 252 (2006) 6394.
29. E.E. Oguzie, *Mater. Chem. Phys*.87 (2004) 212.
30. E.E. Oguzie, *Mater. Letts*. 59 (2005) 1076.
31. E.E. Ebenso, P.C. Okafor, U.J. Ibok, U.J. Ekpe, A.I. Onuchukwu, *Jour. Chem. Soc. Nig*. 29 (2004) 15.
32. E. E. Ebenso, *Bull. Electrochem*. 19 (2003) 209.
33. E. E. Ebenso, *Bull. Electrochem*. 20 (2004) 551.
34. E.E. Oguzie, C. Unaegbu, C.N. Ogukwe, B.N. Okolue, A.I. Onuchukwu, *Mater. Chem. Phys*. 84 (2004) 363.
35. E.E. Oguzie, B.N.Okolue, C.N. Ogukwe, C. Unaegbu, *Mater. Letts.* 60 (2006) 3376.
36. E.E. Ebenso, E.E. Oguzie, *Mater. Letts.* 59 (2005) 2163.
37. E.E. Oguzie, B.N. Okolue, E.E. Ebenso, G.N.Onuoha, A.I. Onuchukwu, *Mater. Chem. Phys*. 87 (2004) 394.
38. E.E. Oguzie, G.N. Onuoha, A.I. Onuchukwu, *Mater. Chem. Phys*. 89 (2005) 305.
39. E.E.Oguzie, E.E. Ebenso, *Pigment. & Resin. Technol*. 35 (2006) 30.
40. S.S. Al-Juaid, Port. *Electrochimica Acta* 25 (2007) 363.
41. J. E. Del Bene, M.J.T. Jordan, *J. Mol. Struct (Theochem)*, 573 (2001) 11.
42. A.D. Becke, *J. Chem. Phys*. 98 (1993) 5648.
43. P. Senet, *Chem. Phys. Lett*. 275 (1997) 527.
44. P. Perez, R. Contreras, A. Vela, O. Tapia, *Chem. Phys. Lett*. 269 (2007) 419.
45. P. Geerlings, F. De Proft, W. Langenaeker, *Chem. Rev*. 103 (2003) 1793.
46. R.G. Parr, R.G. Pearson, *J. Am. Chem. Soc.* 105 (1983) 7512.
47. Y. Shao, L.F. Molnar, Y. Jung, J. Kussmann, C. Ochsenfeld, S.T. Brown, A.T.B. Gilbert, L.V. Slipchenko, S.V. Levchenko, D.P. O'Neill, R.A. DiStasio Jr., R.C. Lochan, T. Wang, G.J.O. Beran, N.A. Besley, J.M. Herbert, C.Y. Lin, T. Van Voorhis, S.H. Chien, A. Sodt, R.P. Steele, V.A. Rassolov, P.E. Maslen, P.P. Korambath, R.D. Adamson, B. Austin, J. Baker, E.F.C. Byrd, H. Dachsel, R.J. Doerksen, A. Dreuw, B.D. Dunietz, A.D. Dutoi, T.R. Furlani, S.R. Gwaltney, A. Heyden, S. Hirata, C-P. Hsu, G. Kedziora, R.Z. Khalliulin, P. Klunzinger, A.M. Lee, M.S. Lee,

W.Z. Liang, I. Lotan, N. Nair, B. Peters, E.I. Proynov, P.A. Pieniazek, Y.M. Rhee, J. Ritchie, E. Rosta, C.D. Sherrill, A.C. Simmonett, J.E. Subotnik, H.L. Woodcock III, W. Zhang, A.T. Bell, A.K. Chakraborty, D.M. Chipman, F.J. Keil, A.Warshel, W.J. Hehre, H.F. Schaefer, J. Kong, A.I. Krylov, P.M.W. Gill and M. Head-Gordon, *Phys. Chem. Chem. Phys.*, 8 (2006) 3172.
48. E.S. Ferreira, C. Giancomelli, F.C. Giacomelli, A. Spinelli, *Mater. Chem. Phys*. 83 (2004) 129.
49. W.H. Li, Q. He, C.L. Pei, B.R. Hou, *J. Appl. Electrochem*. 38 (2008) 289.
50. A.A. Hermas, M.S. Morad, M.H. Wahdan, *J. Appl. Electrochem*. 34 (2004) 95.
51. S.S. Abdel Rehim, H.H. Hassan, M.A. Amin, *Appl. Surf. Sci*. 187 (2002) 279.
52. C. Deslouis, G. Maurin, N. Pebere, B. Tribollet, *J. Appl. Electroc*hem. 18 (1988) 745.
53. S. K. Shukla, M.A. Quraishi, *Corros. Sci.* 51 (2009) 1990.
54. K. Juttner, *Electrochim. Acta*, 35 (1990) 1501.
55. W.R. Fawcett, Z. Kovacova, A. Motheo, C. Foss, *J. Electroanal. Chem*. 326 (1992) 91.
56. F. Mansfeld, *Corros*. 36 (1981) 301.
57. J.R. Mcdonald, *J. Eectroanal. Chem*. 223 (1987) 25.
58. J. Pang, A. Briceno, S. Chander, *J. Electrochem. Soc*. 137 (1990) 3447.
59. U. Rammelt, G. Reinhard, *Corros. Sci*. 27 (1987) 373.
60. A.K. Singh, M.A. Quraishi, *J. Appl. Electrochem*. 41 (2011) 7.
61. H.H. Hassan, *Electrochim, Acta*, 51 (2006) 5966.
62. A. Fedorov, Y. N. Zhuravlev., V. P. Berveno. *Phys. Chem. Chem. Phys*., 13 (2011) 5679.
63. N. O. Eddy, S. R. Stoyanov, E. E. Ebenso, *Int. J. Electrochem. Sci*., 5 (2010) 1127.
64. R.G. Pearson, *Proc. Nati. Acad. Sci*. USA, 83 (1986) 8440.
65. W. Li, Q. He, C. Pei, B. Hou, *Electrochim. Acta* 52 (2007) 6386
66. P. Fuentealba, P. Perez, R. Contreras, *J. Chem. Phys*. 113 (2000) 2544.